Resembled Tactile Feedback for Object Recognition Using a Prosthetic Hand

Luis Vargas , He Huang, Senior Member, IEEE, Yong Zhu, Senior Member, IEEE, Derek Kamper, Member, IEEE, and Xiaogang Hu, Senior Member, IEEE

Abstract—Tactile feedback in the hand is essential for interaction with objects. Here, we evaluated how artificial tactile sensation affected the recognition of object properties using a myoelectrically controlled prosthetic hand. Electromyogram signals from the flexor and extensor finger muscles were used to continuously control either prosthetic joint velocity or position. Participants grasped objects of varying shape or size using the prosthetic hand. Tactile feedback was evoked by transcutaneous nerve stimulation along the participant's upper arm and modulated based on the prostheticobject contact force. Multi-channel electrical stimulation targeted the median and ulnar nerve bundles to produce resembled tactile sensations at distinct hand regions. The results showed that participants could gauge the onset timing of tactile feedback to discern object shape and size. We also found that the position-controller led to a greater recognition accuracy of object size compared with velocity-control, potentially due to supplemental joint position information from muscle activation level. Our findings demonstrate that non-invasive tactile feedback can enable effective object shape and size recognition during prosthetic control. The evaluation of tactile feedback across myoelectric controllers can help understand the interplay between sensory and motor pathways involved in the control of assistive devices.

Index Terms—Tactile feedback, prosthetic control, object recognition, transcutaneous nerve stimulation.

I. INTRODUCTION

OMATOSENSORY feedback works in unison with motor function to enable us to perform various daily tasks [1]. Following an amputation, individuals lose both motor and sensory functions, thus limiting their independence and quality of life. In recent years, prosthetic hands have advanced to a degree where the mechatronic design can nearly replicate human hand

Manuscript received 14 July 2022; accepted 28 July 2022. Date of publication 8 August 2022; date of current version 24 August 2022. This letter was recommended for publication by Associate Editor H. Kajimoto and Editor J.-H. Ryu upon evaluation of the reviewers' comments. This work was supported in part by the National Science Foundation under Grants IIS-1954587 and ECCS-2123678, in part by NIDILRR under Grant ARHF19000021, and in part by the National Institute of Health under Grant 1R01HD108473-01. (Corresponding author: Xiaogang Hu.)

Luis Vargas, He Huang, Derek Kamper, and Xiaogang Hu are with the Joint Department of Biomedical Engineering, University of North Carolina-Chapel Hill and NC State University, Raleigh, NC 27695 USA (e-mail: lgvargas@ncsu.edu; hhuang11@ncsu.edu; dgkamper@ncsu.edu; xiaogang@unc.edu).

Yong Zhu is with the Mechanical and Aerospace Engineering Department, NC State University, Raleigh, NC 27695 USA (e-mail: yzhu7@ncsu.edu).

This work involved human subjects or animals in its research. Approval of all ethical and experimental procedures and protocols was granted by the Institutional Review Board of the University of North Carolina at Chapel Hill under Application No. 16-1852, and performed in line with the Declaration of Helsinki.

Digital Object Identifier 10.1109/LRA.2022.3196958

motions [2]. Although these current devices have the potential to alleviate motor deficits in arm amputees, intuitive control of prostheses is still limited, in part due to the lack of sensory information [3]. Tactile feedback from our fingertips helps convey contact force magnitude and direction. Without tactile cues, individuals with an amputation must rely on auditory or visual cues, leading to cumbersome prosthetic control [4]. In addition, prior work suggests that visual feedback alone is not sufficient to compensate for the loss of tactile feedback, and this can lead to low user confidence [5]. As a result, the lack of somatosensory feedback is deemed one of the primary reasons for prosthesis abandonment [6].

Natural biological tactile percepts are evoked from mechanoreceptors in our skin [7]. Various mechanoreceptors work together to convey intricate percepts based on the stimulus frequency, location, and intensity [8]. For individuals with an amputation, artificial sensations can be evoked through invasive and non-invasive platforms to resemble somatosensory cues, allowing users to associate stimuli to real-time finger force or joint angle information [9], [10]. Although different stimulation approaches provide users with informative feedback, these approaches can be limited based on the type of sensation. For instance, non-somatotopic percepts may impose greater cognitive burden during stimuli interpretation, due to the dissimilarity in location and/or modality [11]. Somatotopic percepts can potentially improve sensation intensity/location discrimination accuracy [12]. Unfortunately, somatotopic percepts are primarily elicited via invasive stimulation of peripheral nerves [13], which can limit wide applications. Alternatively, somatotopic percepts can be elicited non-invasively by activating sensory axons in the nerve trunk via transcutaneous nerve stimulation (TNS) [14], [15]. Although non-invasive nerve stimulation shows promise, its efficacy across different myoelectric controllers has not been fully investigated.

To enable effective closed-loop prosthetic control, it is vital that we recognize the complex relations between the sensory and motor components of prosthetic control. Action-perception coupling during prosthetic use can affect sensory feedback integration, potentially impacting overall system functionality [16]. Continuous myoelectric controllers typically map the level of muscle activation to the velocity or position of the prosthetic joints. Contradictory results have been reported when comparing performance outcomes during velocity and position control [17], [18]. One study suggested that velocity control may be more efficient for operating the prosthesis; however, position control allows greater fine manipulation of objects [19]. As a result, it is essential to discern how non-invasive

2377-3766 © 2022 IEEE. Personal use is permitted, but republication/redistribution requires IEEE permission. See https://www.ieee.org/publications/rights/index.html for more information.

fingertip tactile feedback and different myoelectric controllers affect the perceptibility of an evoked sensation; this has only been explored in a few studies [9], [10].

Accordingly, the purpose of the current study was to evaluate how artificial tactile sensation affected the recognition of object properties when the prosthetic hand was controlled via two distinct myoelectric controllers. Able-bodied subjects controlled a prosthetic hand using position or velocity control. The electromyogram (EMG) signals from flexor/extensor hand muscles were mapped to desired prosthetic joint positions or velocities. During prosthetic control, prosthetic fingertip forces modulated tactile percepts to discern the shape or size of the grasped objects. Tactile feedback was elicited by activating axons in the median/ulnar nerves via an electrode grid placed on the upper arm. As electrical stimulation was sent to different electrode pairs, different axons were recruited, producing different localized hand sensations [20]. Prior work showed that shape recognition via two independently modulated hand sensations through two channels of stimulation in open-loop configurations [21]; however, it has yet to be determined whether the information can be utilized for object recognitions during myoelectric control of a prosthetic hand. In addition, prior work has shown that size recognition can be performed with multi-modal tactile and proprioceptive cues [10]. Earlier work showed that, with position control, users can control prosthetic finger positions in a reasonable accuracy without vibrotactile feedback, because users can use the intrinsic proprioceptive cues when muscle activation levels are directly associated to the prosthetic joint angle [10], [18], [22]. We hypothesized that, compared with velocity control, position control would lead to higher recognition accuracy, because a direct mapping of muscle activation level to joint position could allow to gauge the joint angle, which could benefit object recognition when paired with tactile feedback. Overall, this non-invasive somatotopic tactile feedback approach allows for the assessment of different effects of myoelectric controllers on object recognition.

II. MATERIALS AND METHODS

A. Participants

Eight able-bodied participants (3 Female, 24-38 years of age) were recruited for this study. All participants gave informed consent via protocols approved by the Institutional Review Board of the University of North Carolina at Chapel Hill (Approval#: 16-1852). Participants had no prior experience with this sensory feedback approach or controlling a prosthetic hand.

B. Experimental Setup

Each participant was seated in front of a table with their right arm placed atop it. The medial portion of their upper arm was cleaned using alcohol pads in preparation for the placement of the stimulation grid. The 2×8 grid, consisting of 1-cm diameter Ag/AgCl gel-based electrodes, was used to elicit sensory percepts via TNS. This grid was positioned just below the short head of the biceps brachii (Fig. 1), which allowed the best transcutaneous access to the median and ulnar nerves. Through the selection of distinct electrode pairs, electrical stimulation created unique electric fields that activated different groups of sensory axons. As a result, haptic sensations at distinct hand

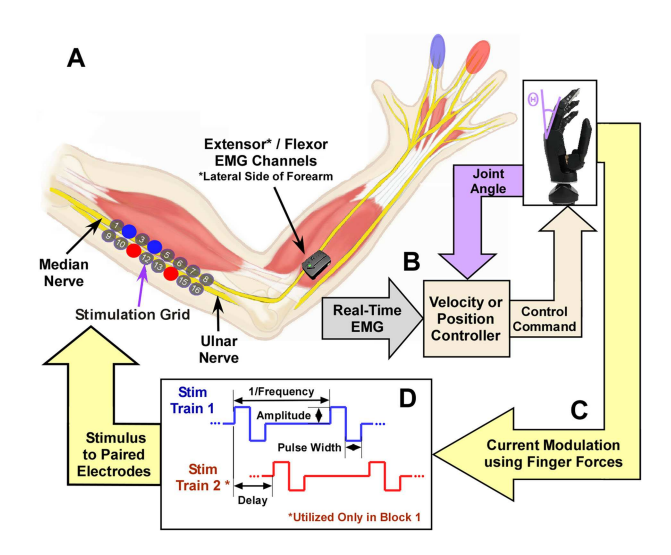


Fig. 1. The placement of the 2x8 stimulation grid and the EMG channels along the participant's arm is depicted (a). Prosthetic movement was monitored and controlled using the EMG recordings and finger joint angles via a velocity or position controller (b). Fingertip forces were used to close the loop providing users with haptic feedback. Graded tactile sensations along the hand were evoked by altering the current amplitude of the delivered biphasic stimulation train (d) Based on the prosthetic's recorded index and middle finger forces (c).

regions could be evoked [20]. A plastic vice placed around the upper arm applied mild inward pressure to stabilize electrodeskin contact. Stimulation current delivered to a single electrode pair can evoke tactile sensation along an individual's hand. Prior work has also shown that stimulating two electrode pairs concurrently (dual-channel stimulation) can elicit more complex resembled sensation regions from individual stimulation locations [21], [23]. Single or dual-channel stimulation was used to elicit complex graded fingertip tactile percepts based on real-time prosthetic grasp forces.

A custom MATLAB script (v2017b, MathWorks, Inc.) controlled the stimulation patterns and electrode pairs. The electrode pair selection was executed using a switch matrix (Agilent Technologies). For each stimulation channel, the switch matrix linked the cathode and anode of an electrical stimulator (STG4008, Multichannel System) to an electrode pair. The stimulator delivered biphasic, charge-balanced, square-wave currents (Fig. 1(d)) using a constant frequency of 150 Hz and pulse width of 200 μ s [24]. A single electrode pair was used for object size detection, while two non-overlapping electrode pairs (i.e., dual channel) were used for shape recognition. A 3.33-ms delay between the two channels was implemented to minimize electric field interference during shape recognition [23].

Stimulation amplitude was altered in real-time based on the fingertip forces from the i-limb prosthetic hand (Ossur). The prosthetic index and middle fingertip forces were recorded using force sensitive resistors (FSR) positioned on the corresponding prosthetic fingertip. Index finger forces were used during both single and dual channel stimulation, while middle finger forces were only used during dual-channel stimulation. A participant-specific and electrode pair-specific sigmoid function was used to transform each fingertip force to a designated stimulation amplitude. The function for each pair was built using an allowable stimulation range, minimum and maximum force, and steepness value [15]. The stimulation range of each pair

Subject #	Prosthetic Finger (Index or Middle)	Evoked Sensation Region (I: Index, M: Middle, R: Ring, P: Pinky, T: Thumb)	Electrode Pair (Cathode - Anode)	Sensory Threshold - Just Below Motor Threshold (mA)
1	Index	I, M & R	3-5	3.2 - 4.1
	Middle	P	4-6	3.3 - 3.8
2	Index	I & M	13-15	1.3 - 1.8
	Middle	R	10-12	1.6 - 2.1
3	Index	I & T	2-4	2.6 - 3.5
	Middle	M & R	6-15	2.6 - 3.7
4	Index	I & M	4-6	2.9 - 4.6
	Middle	M & R	13-15	3.0 - 3.9
5	Index	I & M	3-7	3.5 - 4.9
	Middle	R & P	10-12	3.3 - 4.3
6	Index	I	6-13	1.6 - 2.2
	Middle	M & R	5-7	2.3 - 3.0
7	Index	I & M	3-5	3.4 - 4.0
	Middle	R	4-6	3.0 - 3.5
0	Index	I, M, & T	5-12	5.0 - 6.7

TABLE I
ELECTRODE PAIRS AND SENSATIONS ELICITED FOR EACH PARTICIPANT

was bounded by the Sensory-Threshold and Just-Below-Motor-Threshold. The Sensory-Threshold is defined as the stimulation amplitude that initially evoked a perceivable tactile sensation along the participant's finger(s). The Motor-Threshold is the stimulation amplitude that first induces finger motion and was initially identified via experimenter's visual detection of evoked finger twitch. For the process, the stimulation amplitude was increased using a step of 0.1 mA. This process was repeated three times, and the outcomes were then averaged as the thresholds. For the upper limit, an amplitude approximately 0.2 to 0.3 mA below the Motor-Threshold was used to avoid muscle activation (Just-Below-Motor-Threshold). Using these two thresholds, the sigmoid function was created using the following function:

R & P

5.3 - 8.6

Middle

$$I(F) = \frac{(I_{Max} - I_{Min})}{1 + \exp\left(-k * \left(F - \frac{F_{Max} + F_{Min}}{2}\right)\right)} + I_{Min}$$

where I, $I_{\rm Max},$ and $I_{\rm Min}$ represent the actual current, Just-Below-Motor-Threshold, and Sensory Threshold, respectively. Steepness, actual force, maximum force, and minimum force were represented by k, F, $F_{\rm Max}$, and $F_{\rm Min}$, respectively. To account for potential force sensor drift, the minimum force was set to 0.5 N, ensuring that stimulation was not evoked prior to object contact. Prior to the experiment, the sigmoid functions were tested by applying pressure to the prosthetic's fingertip sensors to ensure that the lower values evoked perceivable sensations, while the upper values did not evoke unintended muscular responses identified via EMG signals. If either value was inadequate, the stimulation range was altered, and the test was completed again. The stimulation ranges for each participant are depicted in Table I. Since the sigmoid function naturally flattens near the upper bound, it minimized the potential for adverse muscle activation. During prosthetic use, the stimuli were updated at 40 Hz based on the force recordings.

During an initial exploration phase, the participants were given the opportunity to explore the tactile feedback and the functionality of the controllers, and the participants can visually see the prosthetic hand. This could help the participants to associate the prosthetic movement to their muscle activation to

improve user intuition. After the exploration phase, the prosthetic hand was placed on a stand and positioned outside of the participant's line of sight to minimize incidental feedback (motor vibration and visual cues) during prosthetic use. In addition, noise-cancelation headphones were used to block the motor's audio cues. During single-channel stimulation for object size recognition, only the prosthetic index finger was controlled. In contrast, both index and middle fingers were controlled during dual-channel stimulation for shape recognition. The prosthetic finger(s) were controlled by the participants using two EMG electrodes (Delsys Trigno). One electrode was placed on the anterior side of the forearm to record the activation of the flexor digitorum superficialis, while the other electrode was placed on the posterior side of the forearm to record from extensor digitorum communis (Fig. 1). Electrode positioning was performed via muscle palpitation. The skin was cleaned using alcohol pads prior to electrode placement. The EMG signals were amplified by 300 and band-pass filtered between 20-450 Hz prior to sampling at 5000 Hz.

The EMG signals were processed to characterize the user intent. The activation level from each muscle was estimated by the rectified and filtered EMG signals using a 200-ms moving window with a 100-ms overlap. The resulting values were then normalized by the peak value recorded during maximum voluntary contraction (MVC) for each muscle.

The resulting relative activation level was mapped to a joint velocity or position in real-time. The reference joint position (P) used in position control was:

$$P = (A_{Max} - A_{Min}) * \left(\frac{EMG_F}{0.5 * MVC_F} - \frac{EMG_E}{0.5 * MVC_E}\right),$$

where A_{Min} and A_{Max} are the minimum (0°) and maximum (85°) joint angles, EMG_F and EMG_E are the activation levels of the flexor and extensor, respectively. Velocity control mapped the joint velocity to the activation level of flexor or extensor. The reference joint velocity (V) for velocity control was:

$$V = (V_{Max} - V_{Min}) * \frac{EMG_{Dir}}{0.5 * MVC_{Dir}},$$

where V_{Min} and V_{Max} are the minimum (25°/s) and maximum (80°/s) joint velocity, and Dir is Flex or Ext, whichever has a greater normalized activation level. The approach ensured a short latency when switching movement directions. The maximum joint angle or velocity corresponded to 50% MVC to minimize potential muscle fatigue, 2% MVC was required to initiate the prosthetic hand movement. A minimum activation of 2% MVC was used to minimize premature prosthetic movement, while ensuring no perceivable delay. The recorded metacarpophalangeal joint angles from the prosthetic index and middle fingers were linked and integrated into a custom proportional-derivative (PD) controller to monitor the finger position or velocity. Control commands to the prosthetic motors were updated at 40 Hz, while the reference position or velocity was updated based on the user intent at 10 Hz.

C. Experimental Procedures

Electrode grid exploration was performed to pinpoint two pairs that elicited sensations at distinct hand regions. For the first pair, sensations along the index finger were found, while an

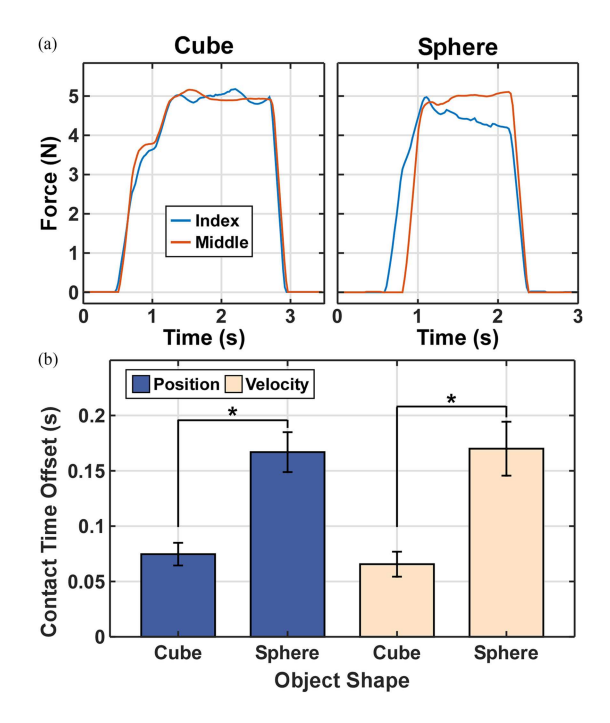


Fig. 2. Example force traces of the prosthetic hand's index (blue) and middle (orange) fingers when grasping a cube and sphere (a). The average contact time offsets of the two shapes for both controllers (b). The error bars indicate standard error, while '*' denotes significant differences in contact time offsets across object shapes.

electrode pair evoking sensation at an alternative region corresponding to the prosthetic middle finger was chosen for the second pair. Once the two pairs were found, the stimulation ranges were identified, and their sigmoid functions were constructed (Table I). Finally, participants were given 3-5 minutes for the position and for the velocity controllers to practice manipulating the prosthetic index and middle fingers by flexing and extending their finger muscles.

The two controllers were presented in discrete blocks. The order of which was randomized for each participant. First, object shape recognition was executed using two shapes with similar sizes: one cube and one sphere. Object shape was encoded based on the temporal difference in object contact for the index and middle fingers; this was termed the contact time offset (Fig. 2(b)). Dual stimulation was employed here. Second, object size recognition was performed using single-channel stimulation. Only the index finger was controlled as the prosthesis grasped three cubes of varying sizes (2, 4, or 6 cm). Object size recognition was encoded based on the time between movement initiation and object contact, because the prosthesis always started from the same extended posture. Participants completed 5 trials per object, resulting in 10 trials per object shape and 15 trials per object size. During these trials, participants were not given feedback about their responses. Example force and/or joint angle traces during object shape and object size tasks are shown in Figs. 2 and 3, respectively.

D. Data Processing

We first calculated the recognition accuracy. Confusion matrices were constructed to compare the ground truth to the perceived object property under each controller. For object shape

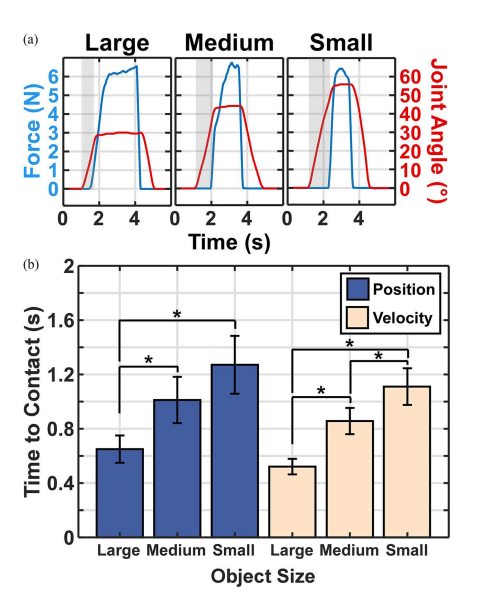


Fig. 3. Example index finger force (blue) and joint angle (red) traces when grasping objects of varying sizes (a). The average time to contact for each object size for both controllers (b). The error bars indicate standard error, while '*' denotes significant differences in time to contact across object sizes.

recognition, the contact time offset between fingers was also computed for each object shape. The offset was calculated as the difference in time when the index and middle fingers produced forces greater than 0.5 N. In addition, the difference in average contact timing between two shapes was calculated for each participant, and the correlation between these values and the recognition accuracy was calculated. For object size recognition, the time to contact was calculated as the time between the movement initiation and a fingertip force greater than 0.5 N. A difference in time to contact across object sizes was evident for both controllers (Fig. 3(b)). 0.5 N was used to calculate the contact time offset and time to contact, because sensory percepts were initially evoked once the fingertip forces surpassed this force level. In addition, to determine if intrinsic proprioceptive feedback during muscle activation improved size recognition accuracy during position control, the level of flexor and extensor activation was computed during the holding period of object size grasp. Specifically, the rectified EMG signals were averaged across the object holding phase. The average flexor and extensor activation levels were then normalized by the MVC of each muscle. For each participant, the normalized activation levels were then averaged among trials with similar size and controller as:

$$\overline{EMG_{X_{All}}} = \frac{1}{n} * \sum_{i=1}^{n} \frac{\overline{EMG_{X_i}}}{MVC_i},$$

where X is position- or velocity-control, i is the trial number, \overline{EMG}_{X_i} is the average EMG across the object holding phase of the trial, and n is the number of trials. To compare across object sizes, ratios of the computed average activation levels were calculated. These ratios were then transformed using a logarithmic transformation for statistical analysis, as:

$$\log (Ratio \ of \ Activation) = \log \frac{\overline{EMG_A}}{\overline{EMG_B}} \ ,$$

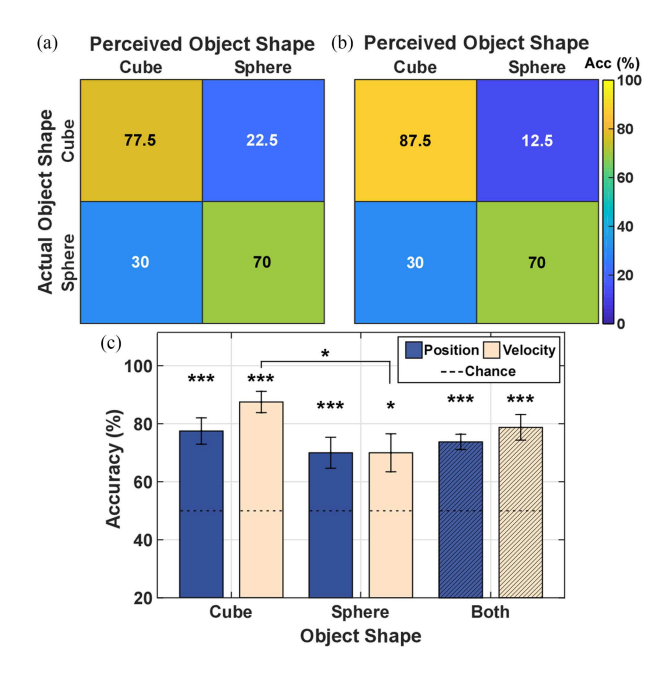


Fig. 4. Confusion matrices denoting the actual and perceived object shape when using position (a) and velocity control (b). The average accuracy across participants is shown (c) With the error bars indicating standard error. '*' denotes p < 0.05 and '***' denoting p < 0.001 when comparing across conditions or comparing accuracies to the chance value.

where *A* and *B* correspond to the normalized activation levels when grasping two distinct object sizes.

E. Statistical Analysis

For all accuracy values, a logarithmic transformation was performed to normalize the outcomes prior to conducting a one sample *t*-test to determine whether accuracy was greater than chance. A chance value of 0.5 and 0.33 was used for object shape and size recognition, respectively. Next, two-way repeated measures analysis of variance (ANOVA) were performed to assess possible differences in accuracy across the controllers and object properties. For the ratios of muscle activation levels, one sample *t*-tests were performed to evaluate whether these values were different from 0 (i.e., log (1)), denoting if the muscle activation differed across object sizes.

III. RESULTS

We first assessed the performance accuracy during object shape recognition under different controllers. The confusion matrices (Fig. 4) assess the perceived object shape in relation to the ground truth. The results showed that most of the grasped objects were correctly identified during both position and velocity control. Specifically, position and velocity control resulted in recognition accuracies of $73.8\% \pm 2.5\%$ and $78.6\% \pm 4.0\%$, respectively. The ANOVA showed a significant main effect across object shapes (F = 6.44, p = 0.017) with a significant difference in accuracy during velocity control (p = 0.028). No main effect across controllers or interaction effect was noted. Most shape recognition accuracies were found to be significantly greater than chance (p < 0.001 for all conditions, except for the Velocity-Sphere condition: p = 0.018).

Fig. 5 highlights the distribution of the contact time offset when grasping the cube and sphere with the two controllers. The

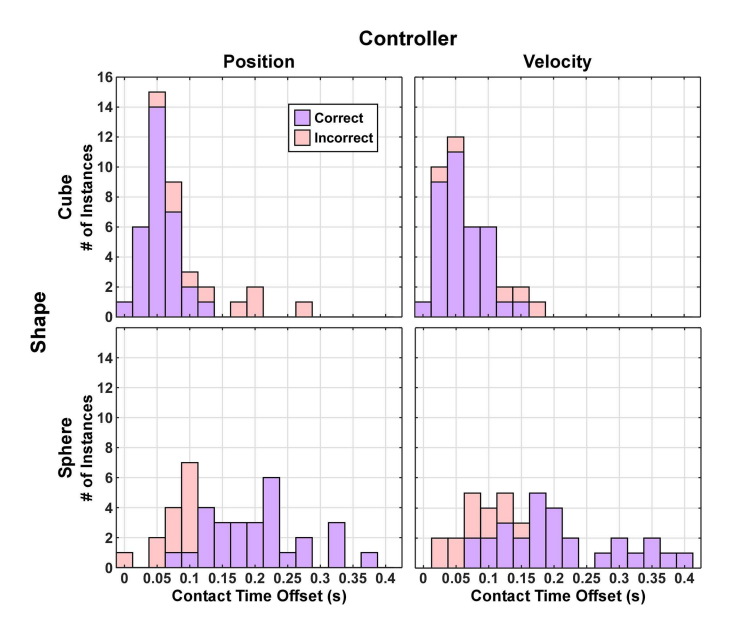


Fig. 5. Histogram of the contact time offset when correctly and incorrectly identifying the cube and sphere during position and velocity control.

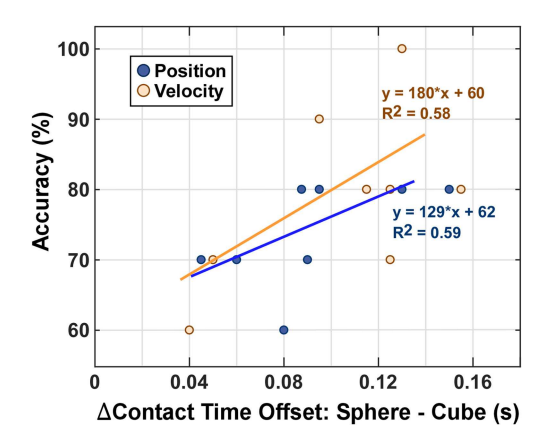


Fig. 6. Object shape recognition accuracy in relation to the difference in contact time offset between the two shapes during position and velocity control.

histogram depicts the offset variability during active prosthetic control across trials and participants. Overall, the histograms showed that the two shapes were incorrectly identified most often when the contact time offset differed from the norm. When evaluating the effects of contact time offset, Fig. 6 displays the recognition accuracy as a function of the difference in contact time offset across object shapes for each participant. As the difference in contact time increases by moving the fingers slowly, the object shape recognition accuracy increases with a moderate correlation.

Next, we evaluated the object size recognition accuracy when employing position and velocity control. The confusion matrices in Fig. 7 illustrate the perceived and actual object size across all participants. The ANOVA showed significant main effects for both controllers and object sizes (Controllers: F = 10.54, p = 0.002; Sizes: F = 6.89, p = 0.003) with significant differences for the medium object across controllers (p = 0.026) and across the medium-small pairwise comparison in velocity control (p = 0.007). No interaction effect was observed. The t-test results also showed that both position and velocity control could be used to discern object size with accuracies greater than chance

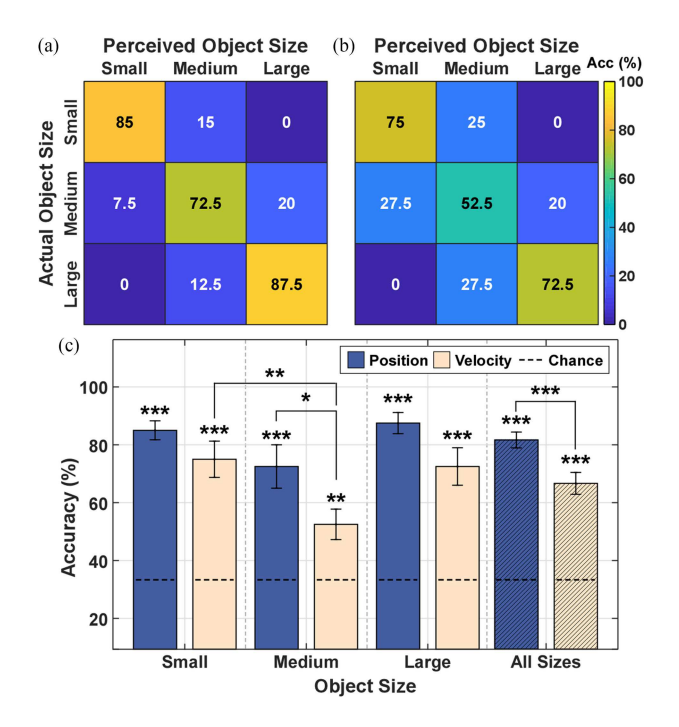


Fig. 7. Confusion matrices of the actual and perceived object size when using position (a) and velocity control (b). The average accuracy across participants is shown (c) With the error bars indicating standard error. '*' denotes p < 0.05 '**' denotes p < 0.01, and '***' denotes p < 0.001 when comparing accuracies to the chance value and across conditions.

(p<0.001 for all conditions, except for the Velocity-Medium condition: p = 0.003). Moreover, object sizes could be discerned during position and velocity control with accuracies of 81.6% \pm 2.6% and 66.7% \pm 3.5%, respectively. We also found that the accuracy was lower using velocity control when compared to position control (p<0.001).

Although significant differences in time to contact were noted for both controllers, when assessing the amount of flexor activation for each controller, not all conditions were found to be distinct across object sizes (Fig. 8). Specifically, during position control, the flexor activation in all three comparisons across object sizes were found to be significantly different (p<0.01). Namely, the flexor muscle activation level differed when grasping different object sizes using position control. However, no significant difference (p>0.05) was observed when comparing the ratios of extensor activation across object sizes for either controller.

IV. DISCUSSION

This study revealed that non-invasive tactile feedback from multi-channel stimulation allowed participants to discern two distinct object shapes and three object sizes using a myoelectric prosthetic hand. In addition, the outcomes depicted how different control schemes impact recognition accuracy. We found that participants could effectively use the evoked tactile feedback to correctly identify object shape and size, when using either position- or velocity-control. We also found that participants could recognize object size more accurately when employing position control than velocity control. These results demonstrate that non-invasive somatotopic tactile feedback can be effectively integrated with prosthetic hands, fostering bidirectional closed-loop control. The outcomes also characterize the

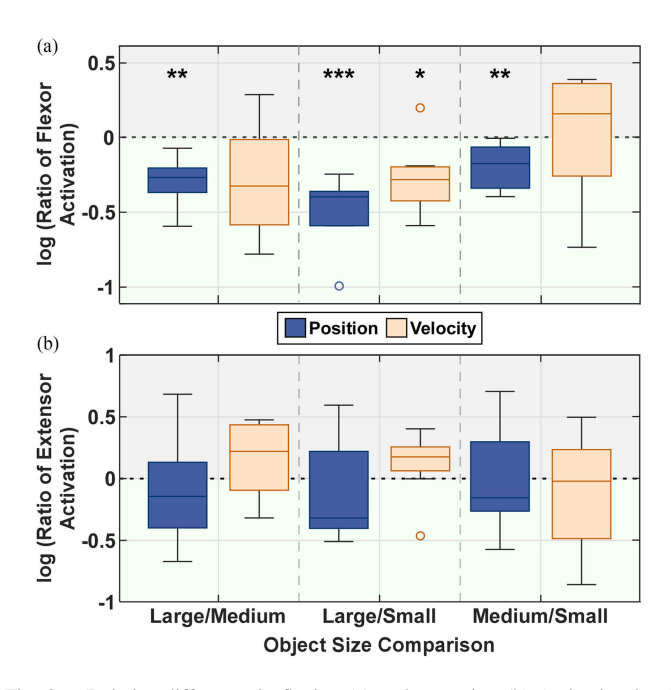


Fig. 8. Relative difference in flexion (a) and extension (b) Activation level across object sizes using position and velocity controllers. Significance is shown with '*' denoting p < 0.05, '**' denoting p < 0.01, and '***' denoting p < 0.001, when comparing to zero, i.e., $\log{(1)}$.

interplay between sensory and motor modules during prosthesisobject interactions, which can help improve our understanding of action-perception coupling in prosthetic control and promote the utility of assistive devices.

Our results showed that object shape recognition could be readily achieved via tactile feedback during myoelectric prosthetic control. Similar recognition accuracy values were observed across position and velocity control conditions. During the task, sensory feedback only occurred when the prosthetic hand reached the object. The perception of tactile feedback can occur without interfering with EMG control. The similarity in recognition accuracy may also be due to the simplicity of the task, involving only two objects. For both controllers, the results showed that the contact time offset was similar, further justifying the similarity in performance. The object contact time offset (Fig. 5) was significantly different across the two shapes for both controllers as well, indicating that the temporal difference could be distinguished by the participants. The results also showed that as the difference in contact time offset increased, the performance accuracy increased. The correlation between contact time offset and recognition accuracy has been reported in prior work as well when employing an experimenter-controlled prosthetic hand [21] or using a simulated grasp trajectory [25]. Finally, the selected refresh rate (40 Hz) for the PD controller and tactile feedback may also contribute to the reduced accuracy when the contact time offset is reduced. Future work will evaluate the impact of controller and feedback update rates on object recognition performance.

Although significant differences from the chance value are noted, the accuracy is not necessarily high given the participants were expected to distinguish only two object shapes. The use of additional object shapes would likely alter the outcomes. When compared with prior studies, the accuracies are slightly lower in the current study, potentially due to several factors.

The first factor is the magnitude of the contact time offset. In prior work, the temporal delay between finger contact could be longer than 1.5 seconds [25], [26]. As shown in the current study (Fig. 6), a longer offset can improve the shape recognition accuracy. A shorter contact time offset in the current study may be caused by increased joint movement speeds. As the prosthesis can move at relatively fast speeds, a slower prosthetic speed regulation may help users to better distinguish the grasped object. Secondly, the employed controllers may affect the outcomes as well. In the current study, continuous velocity and position controllers were evaluated. The use of a discrete state-based controller using pattern classification may minimize the variability in movement speeds as well as the contact time offset. Thus, the discrete state-based controller could potentially improve the object recognition accuracy [21], [25], [27]. Lastly, additional training could improve the stimuli perceptibility. In the current study, only a brief training was provided. Future work should be performed to evaluate how training can impact object recognition accuracy.

Our results also showed that object size recognition could be performed using tactile feedback. Contrary to object shape recognition, differences were observed between the two controllers for size recognition. Our findings showed that greater recognition accuracy was achieved during position control than during velocity control. When evaluating the time to contact, velocity control results in times that were significantly different across object sizes; however, not all comparisons were significant in contact times for position control (Fig. 3(b)), yet greater recognition accuracy were observed. It is possible that the difference in accuracy is due to the use of intrinsic proprioceptive cues (muscle activation level) during position control, and its direct association with the prosthetic joint angle. Similar conclusions were observed with invasive peripheral nerve stimulation [18]. This is further justified based on the significant differences in flexor muscle activation across object sizes. The proprioceptive cue potentially alleviated the lack of significance in time to contact during position control. In prior work, object size recognition involving solely tactile feedback also resulted in similar outcomes; although slight differences in accuracy were likely due to the number of different-sized objects and variations in velocity of the joint during experiment [18], [28]. One limitation of our experimental setup involves the use of a set starting posture. As a result, the relative time to contact is correlated to object size. If the starting posture is altered, the relative differences may be similar, but the absolute timings would be futile, because the reference position is lost. This would require the participants to rely more on proprioceptive feedback.

Although position control benefits from these intrinsic proprioceptive cues, position control requires continuous muscular activation to maintain the joint position, making participants more prone to fatigue. Implementing a holding state during position control can potentially reduce the need for sustained muscle activation and delay fatigue onset [29]. Nonetheless, studies have shown that task performance is similar across controllers when proprioceptive feedback is provided [10], [22]. Recent work concluded that object size recognition accuracy is improved when users are given both tactile and proprioceptive cues [28]. The use of both sensory cues has also enabled the recognition of multiple object properties simultaneously [10], [28], [30]. Recent studies have also developed new techniques

to improve prosthetic control by providing proprioceptive cues [22], [31], [32]. Although it can be beneficial to provide rich sensory information, it is important to note that as the number of feedback sources increases so does the difficulty interpreting numerous sensory perceptions simultaneously. Further evaluations on the integration of multi-modal feedback strategies should be performed to enhance user intuition and optimize the quality, quantity, and cognitive cost of future feedback strategies.

The non-invasive nature of this somatotopic tactile feedback technique can promote the closed-loop evaluation of current and future assistive devices. Although these tests involved a single prosthetic hand, other assistive or teleoperative devices may also benefit from this evaluation. In addition, this non-invasive approach can be implemented in alternative settings, involving individuals with sensory deficits. Prior work suggest that, even when the motor system is unimpaired, a lack of tactile feedback can negatively impact task performance [33]. Overall, the integration of sensory feedback across these alternative settings can possibly improve a person's quality of life. Nonetheless, future tests should examine the role that artificial feedback plays in these scenarios.

A few technical limitations include the potential applications for the current sensory-motor configuration (EMG sensor and stimulation setup) and the indirect pairing of the evoked sensory regions to only two prosthetic fingers. The current placement of the stimulation grid promotes its use across various amputation levels. In general, the current system targets individuals with wrist disarticulations or transradial amputations. The stimulation on a proximal position also limits the potential for stimulation artifact on EMG recordings. Earlier work has shown that able-bodied individuals and individuals with an amputation perceive similar tactile feedback through nerve stimulation [20]. It is expected that the outcomes observed in able-bodied participants may be representative of those in individuals with an amputation. Modified sensory feedback strategy is needed to translate this approach to individuals with higher levels of amputations. In the current study, we focused more on locating two distinct sensation regions along the hand using two separate electrode pairs rather than locating two pairs that evoked single-finger sensations. In doing so, this study explored whether tactile information can be delivered using two stimulation channels to portray the grasp forces at two distinct regions of the hand during active prosthetic use. Our earlier study has shown that evoked sensations can range from a single finger quadrant to multiple fingers [23]. Overall, the location of the electrode grid relative to the median and ulnar nerves as well as the stimulation intensity can alter the specificity of stimulation regions. Nonetheless, the issue of specificity in the current study is a limitation that we need to address in the future with alterative electrode grid configurations and stimulation patterns.

In cases where nerve stimulation may be affected by amputation level, non-somatotopic strategies may provide prosthetic users with sensory information by targeting cutaneous receptors on the skin surface. Although dissimilarity in sensation modality and location initially affects cognitive cost, recent non-somatotopic strategies can evoke beneficial percepts describing grasp force and finger aperture [34], [35]. Increased practice can improve their intuitiveness, allowing users to become better acquainted with the evoked sensations. Studies have shown that training can improve the perceptibility of a stimuli's strength

and location [36] and lead to intuitive discrepancy of these sensations when compared to somatotopic approaches, [37]. Non-somatotopic strategies can also provide more flexibility as different tactor types can be applied to various regions depending on the amputation level or the sensory acuity of an individual's residual limb. In addition, a greater number of stimulation sites may convey more information that allows more complex object recognition tasks, if cognitive cost can be alleviated.

V. CONCLUSION

In conclusion, this study shows that transcutaneous nerve stimulation can elicit tactile percepts, enabling object size and shape recognition during the closed-loop control of a prosthetic hand. Evoked tactile feedback could be effectively integrated with both position and velocity controllers, leading to successful perception of object shape and size. A greater success in object size recognition during position control indicates that intrinsic proprioceptive cues may also assist during size recognition. The non-invasive nature of this approach provides a platform to characterize the differences in the intricate action-perception coupling during assistive device utility. Our findings also help us to understand the interactions between the motor and sensory modules of current prosthetic systems, which can help improve assistive device designs.

REFERENCES

- [1] S. J. Bensmaia, D. J. Tyler, and S. Micera, "Restoration of sensory information via bionic hands," Nat. Biomed. Eng., pp. 1-13, Nov. 2020.
- [2] L. Trent et al., "A narrative review: Current upper limb prosthetic options and design," Disabil. Rehabil. Assistive Technol., vol. 15, no. 6, pp. 604-613, Aug. 2020.
- [3] P. Svensson, U. Wijk, A. Björkman, and C. Antfolk, "A review of invasive and non-invasive sensory feedback in upper limb prostheses," Expert Rev. Med. Devices, vol. 14, no. 6, pp. 439-447, Jun. 2017.
- [4] D. J. Tyler, "Neural interfaces for somatosensory feedback: Bringing life to
- a prosthesis," *Curr. Opin. Neurol.*, vol. 28, no. 6, pp. 574–581, Dec. 2015. [5] Y. Ban, T. Narumi, T. Tanikawa, and M. Hirose, "Controlling perceived stiffness of pinched objects using visual feedback of hand deformation," in Proc. IEEE Haptics Symp., 2014, pp. 557-562.
- [6] E. Biddiss, D. Beaton, and T. Chau, "Consumer design priorities for upper limb prosthetics," Disabil. Rehabil. Assistive Technol., vol. 2, no. 6, pp. 346-357, Jan. 2007.
- [7] H. P. Saal and S. J. Bensmaia, "Touch is a team effort: Interplay of submodalities in cutaneous sensibility," Trends Neurosci., vol. 37, no. 12, pp. 689-697, Dec. 2014.
- [8] E. V. Okorokova, Q. He, and S. J. Bensmaia, "Biomimetic encoding model for restoring touch in bionic hands through a nerve interface," J. Neural Eng., vol. 15, no. 6, Oct. 2018, Art. no. 066033.
- Q. Fu and M. Santello, "Improving fine control of grasping force during hand-object interactions for a soft synergy-inspired myoelectric prosthetic hand," Front. Neurorobot., vol. 11, pp. 1-15, Jan. 2018.
- [10] L. Vargas, H. Huang, Y. Zhu, and X. Hu, "Object recognition via evoked sensory feedback during control of a prosthetic hand," IEEE Robot. Automat. Lett., vol. 7, no. 1, pp. 207-214, Jan. 2022
- [11] J. S. Schofield, K. R. Evans, J. P. Carey, and J. S. Hebert, "Applications of sensory feedback in motorized upper extremity prosthesis: A review," Expert Rev. Med. Devices, vol. 11, no. 5, pp. 499-511, Sep. 2014.
- [12] D. Zhang et al., "Somatotopical feedback versus non-somatotopical feedback for phantom digit sensation on amputees using electrotactile stimulation," J. NeuroEng. Rehabil., vol. 12, no. 1, pp. 1-11, Dec. 2015.
- [13] S. Raspopovic, G. Valle, and F. M. Petrini, "Sensory feedback for limb prostheses in amputees," Nat. Mater., vol. 20, no. 7 pp. 925-939, Apr. 2021.
- L. Vargas, H. Huang, Y. Zhu, and X. Hu, "Evoked tactile feedback and control scheme on functional utility of prosthetic hand," IEEE Robot. Automat. Lett., vol. 7, no. 2, pp. 1308-1315, Apr. 2022.
- [15] L. Vargas et al., "Object stiffness recognition using haptic feedback delivered through transcutaneous proximal nerve stimulation," J. Neural Eng., vol. 17, no. 1, Dec. 2019, Art. no. 016002.

- [16] J. W. Sensinger and S. Dosen, "A review of sensory feedback in upper-limb prostheses from the perspective of human motor control," Front. Neurosci., vol. 14, pp. 1–24, Jun. 2020.
- [17] S. Mick et al., "Performance and usability of various robotic arm control modes from human force signals," Front. Neurorobot., vol. 11, pp. 1–16, Oct. 2017.
- [18] J. A. George et al., "Biomimetic sensory feedback through peripheral nerve stimulation improves dexterous use of a bionic hand," Sci. Robot., vol. 4, no. 32, Jul. 2019, Art. no. eaax2352
- [19] S. Patwardhan et al., "Volitional control of target position using sonomyography," Assistive Technol., vol. 33, no. 3, p. 166, May 2021.
- [20] H. Shin et al., "Evoked haptic sensations in the hand via non-invasive proximal nerve stimulation," J. Neural Eng., vol. 15, no. 4, Aug. 2018, Art. no. 046005.
- [21] L. Vargas, H. Huang, Y. Zhu, and X. Hu, "Object shape and surface topology recognition using tactile feedback evoked through transcutaneous nerve stimulation," IEEE Trans. Haptics, vol. 13, no. 1, pp. 152-158, Jan.-Mar. 2020.
- [22] L. Vargas, H. H. Huang, Y. Zhu, and X. Hu, "Closed-loop control of a prosthetic finger via evoked proprioceptive information," J. Neural Eng., vol. 18, no. 6, Dec. 2021, Art. no. 066029.
- [23] L. Vargas, G. Whitehouse, H. Huang, Y. Zhu, and X. Hu, "Evoked haptic sensation in the hand with concurrent non-invasive nerve stimulation.' IEEE Trans. Biomed. Eng., vol. 66, no. 10, pp. 2761-2767, Oct. 2019.
- [24] L. Vargas, H. Huang, Y. Zhu, and X. Hu, "Stiffness perception using transcutaneous electrical stimulation during active and passive prosthetic control," in Proc. IEEE 42nd Annu. Int. Conf. Eng. Med. Biol. Soc., 2020, pp. 3909-3912.
- [25] G. Valle et al., "Sensitivity to temporal parameters of intraneural tactile sensory feedback," J. NeuroEng. Rehabil., vol. 17, no. 1, Dec. 2020, Art. no. 110.
- [26] S. Raspopovic et al., "Restoring natural sensory feedback in real-time bidirectional hand prostheses," Sci. Transl. Med., vol. 6, no. 222, Feb. 2014, Art. no. 222ra19.
- [27] G. Valle et al., "Comparison of linear frequency and amplitude modulation for intraneural sensory feedback in bidirectional hand prostheses," Sci. Rep., vol. 8, no. 1, Dec. 2018, Art. no. 16666.
- [28] E. D'Anna et al., "A closed-loop hand prosthesis with simultaneous intraneural tactile and position feedback," Sci. Robot., vol. 4, no. 27, Feb. 2019, Art. no. eaau8892.
- S. B. Godfrey, M. Bianchi, A. Bicchi, and M. Santello, "Influence of force feedback on grasp force modulation in prosthetic applications: A preliminary study," in $\hat{P}roc.$ IEEE 38th Annu. Int. Conf. Eng. Med. Biol. Soc., 2016, pp. 5439-5442.
- [30] T. J. Arakeri, B. A. Hasse, and A. J. Fuglevand, "Object discrimination using electrotactile feedback," J. Neural Eng., vol. 15, no. 4, Aug. 2018, Art. no. 046007.
- [31] P. D. Marasco et al., "Illusory movement perception improves motor control for prosthetic hands," Sci. Transl. Med., vol. 10, no. 432, pp. 1-13,
- [32] R. Rangwani and H. Park, "A new approach of inducing proprioceptive illusion by transcutaneous electrical stimulation," J. NeuroEng. Rehabil., vol. 18, no. 1, Dec. 2021, Art. no. 73.
- [33] R. S. Johansson, C. Häger, and L. Bäckström, "Somatosensory control of precision grip during unpredictable pulling loads," Exp. Brain Res., vol. 89, no. 1, pp. 204-213, Apr. 1992.
- [34] A. E. Pena, L. Rincon-Gonzalez, J. J. Abbas, and R. Jung, "Effects of vibrotactile feedback and grasp interface compliance on perception and control of a sensorized myoelectric hand," PLoS One, vol. 14, no. 1, pp. 1-21, Jan. 2019.
- [35] M. Guemann et al., "Effect of vibration characteristics and vibror arrangement on the tactile perception of the upper arm in healthy subjects and upper limb amputees," J. NeuroEng. Rehabil., vol. 16, no. 1, pp. 1-16, Dec. 2020.
- [36] H. C. Stronks, J. Walker, D. J. Parker, and N. Barnes, "Training improves vibrotactile spatial acuity and intensity discrimination on the lower back using coin motors," Artif. Organs, vol. 41, no. 11, pp. 1059-1070, Nov. 2017.
- [37] G. Chai, D. Zhang, and X. Zhu, "Developing non-somatotopic phantom finger sensation to comparable levels of somatotopic sensation through user training with electrotactile stimulation," IEEE Trans. Neural Syst. Rehabil. Eng., vol. 25, no. 5, pp. 469-480, May 2017.